Applied Catalysis A: General 391 (2011), 215-224

Adsorption–desorption equilibrium investigations of *n*-butane on nanocrystalline sulfated zirconia thin films

R. Lloyd, T. W. Hansen , W. Ranke, F. C. Jentoft, R. Schlögl

Fritz-Haber-Institut der Max-Planck-Gesellschaft, Departement of Inorganic Chemistry, D-14195 Berlin, Germany

* Corresponding author: e-mail fcjentoft@ou.edu,

Received 16 March 2010; revised 24 May 2010; accepted 15 June 2010. Available online 23 June 2010.

Abstract

Nanocrystalline thin films of the alkane skeletal isomerisation catalyst sulfated zirconia were successfully deposited on a silicon substrate in order to allow the application of surface science techniques. Thermal treatment of the films was optimised to chemically mimic the powder preparation process, resulting in films possessing the essential features (including tetragonal phase, nanocrystallinity and sulfur content of ~3 atomic %) of active powder catalysts. The *n*-butane adsorption–desorption equilibrium under isobaric conditions (10^{-8} to 10^{-6} hPa) over the temperature range 300–100 K was monitored by photoelectron spectroscopy. Analysis of the isobars revealed strong and weak *n*-butane chemisorption sites, releasing heats of between 59–40 and 47–34 kJ/mol, corresponding to 5 and 25% of a monolayer coverage, respectively. The total amount of chemisorbed *n*-butane coincides with the estimated number of surface sulfate groups. An increase in adsorption heat was observed between coverages of ~5–8% of a monolayer, indicating adsorbate–adsorbate interactions. It follows that adjacent sites are present and isomerisation by a bimolecular surface reaction is feasible. Physisorption on the films generates heats of ~28 kJ/mol, for coverages from 30% up to a complete monolayer. Multilayer adsorption results in the formation of an electrically insulating adsorbate structure. It is proposed that the strong chemisorption sites correspond to an interaction with a minority disulfate species.

Keywords: sulfated zirconia, model system, TEM, XPS, UPS, butane, heats of adsorption

1. Introduction

Holm and Bailey were the first to discover the catalytic isomerisation activity of sulfated zirconia (doped with platinum), as documented by their patent of 1962.[1] Hino and Arata reported in 1979 and 1980 the isomerisation of *n*-butane at room temperature on sulfated zirconia.[2,3] Their work initiated a strong interest in the application of this type of material in acid catalysis,[4,5] and commercial use followed.[6] Sulfate is a key component, and numerous propositions of its structure on the zirconia surface have been published, the majority of which were developed with the design of strong Brønsted or Lewis acid sites in mind.[7] Recent experimental and theoretical findings[8,9] have shown that active catalysts possess an IR band at ~1404 cm^{-1}, which is ascribed to the S=O bond stretching vibrations in disulfate or adsorbed SO_3 molecules. These surface species are proposed to initiate alkane conversion by oxidative dehydrogenation. However, a complete picture of the surface sites on sulfated zirconia and their interaction with butane is lacking.

Analysis by surface sensitive techniques, which are now very advanced and routinely applied, may provide more insight. However, the application of these techniques to "real" powder oxide catalysts, such as sulfated zirconia, is often not possible or limited, as the catalysts' porous structures give rise to diffusion limitations and their electrically and thermally insulating nature can cause charge accumulation and temperature gradients. Model systems can be used to overcome these problems. Thin, single-crystalline films grown on conducting substrates have been successfully employed leading to a detailed knowledge of the surface structure and reactivity of oxides.[10,11] For example, Meinel *et al.*[12] prepared single-crystalline cubic sulfated zirconia films by reactive deposition of zirconium onto Pt(111) in an O_2 atmosphere, followed by exposure to a SO_3 atmosphere. During sulfation a ($\sqrt{3}$ x $\sqrt{3}$)R30° structure develops, which is stable to 700 K. The drawbacks of single crystal models are their oversimplifications, for example the lack of defects and support interaction; the transfer of findings to "real" powder catalysts has thus had limited success. Alternatively, model systems may consist

of particles supported on thin oxide or carbon films. The films are deposited on flat, inert, and conducting substrates,[13,14] and significant charge accumulation during experiments can be avoided, even if the film is an insulator. Such materials are inherently more complex than flat, continuous single-crystalline films and better mimic industrial, supported catalysts.

A model for sulfated zirconia can be obtained following De Guire and co-workers[15-17] who developed a method to prepare sulfated zirconia films by chemical deposition of zirconium sulfate from an aqueous acid-stabilised medium on sulfonic acid terminated self-assembled monolayers (SAMs) attached to the oxidised surface of a silicon wafer. Surface morphology studies of such zirconia films found in addition to the film, particles of 200 nm and larger embedded in the film.[18,19] Further development by Fischer and co-workers[20,21] to prevent homogenous deposition, by lowering of the film deposition temperature, resulted in smooth, non-porous, continuous sulfated zirconia thin films. To optimise the deposition conditions the stability of the sulfated zirconia precursor solution was investigated,[22] as well as on the forces between the SAMs and zirconia particles in solution.[23] Pyrolysis of the deposited material in argon produces a polycrystalline layer of tetragonal sulfated zirconia, as shown by transmission electron microscopy (TEM).[24-26] Mechanical properties of sulfated zirconia films prepared from similar aqueous depositions on SAM-covered substrates have also been studied.[27-29]

The interaction of surfaces with gas molecules can be elucidated by adsorption–desorption (A–D) equilibrium measurements. Isotherms or isobars,[30] obtained using flat, conducting surfaces, have been used to deduce coverage-dependent isosteric (constant coverage) heats of adsorption[31] and kinetic data, including the reaction order for desorption and adsorption, the Kisliuk factor and the frequency factor for desorption.[30] Surface sensitive spectroscopic methods, such as X-ray or ultraviolet photoelectron spectroscopy (XPS and UPS), can be used to measure adsorbate coverage under A–D equilibrium conditions. Evaluation of the spectroscopic data can therefore lead to information relating to how the adsorbate binds to the adsorbent, as well as allowing the generation of isobars or isotherms.

UPS measurements under A–D equilibrium have been used to investigate a variety of systems. The Henzler group determined heats of adsorption of water on NaCl(100)[32] and KCl(100).[33] Ranke and co-workers identified adsorption sites and heats of adsorption for ammonia on Ge(001), (113) and (111) surfaces;[30,34] and for water, ethylbenzene and styrene on FeO(111), Fe_3O_4(111) and Pt(111) surfaces.[30,35-37] XP spectra, measured also under adsorption-desorption equilibrium, were used to support the assignments of the various adsorbate states and coverage determinations for water on FeO(111) and Fe_3O_4(111) surfaces.[37] Isosteric heats of adsorption determined for water on FeO(111) and Fe_3O_4(111) are similar in value to heats of desorption deduced from TDS measurements.[37]

The goal of this work is to comprehensively describe the adsorption sites on sulfated zirconia. Thin films are produced, by altering the method described by Fischer,[20,21] and extensively characterised to ensure they are a suitable chemical model. Photoelectron spectroscopy is used to investigate the interaction of *n*-butane with the sulfated zirconia thin films under A–D equilibrium. Low pressures and temperatures are applied as sulfated zirconia is known to be catalytically active even at room temperature.[2] Isobaric studies are performed to identify the various adsorption sites on the films and quantitatively describe how the isosteric adsorption heats of *n*-butane vary with coverage.

2. Experimental

2.1. Synthesis and thermal treatment

Single crystal silicon (100) 1 cm^2 wafers were used as substrates, either p-type, 10 mOhm.cm, 750 μm thick or n-type, 4.2 Ohm.cm, 1.3 mm thick with a groove drilled into the side for thermocouple placement. The silicon wafers were cleaned using chloroform, acetone, ethanol and water, sequentially. Millipore®-filtered water was used for all preparation steps. The silicon wafers were then treated in Standard Clean 1 followed by Standard Clean 2 solutions,[38] both for 40 min at a temperature of 343 K. Oxidation of the wafers was performed in "piranha" solution (3 parts 30% hydrogen peroxide to 5 parts conc. sulfuric acid); at 353 K for 50 min. "Piranha" solution is extremely aggressive and must be handled with caution.

To deposit the SAM, the wafers were immersed in a solution of 50 μl of 1-thioacetato-16-(trichlorosilyl)hexadecane in 5 ml of bicyclohexyl for at least 5 h under an argon atmosphere. The hydrophobic terminal thioacetate group of the SAM was then oxidised in a saturated aqueous solution of $KHSO_5 \cdot KHSO_4 \cdot K_2SO_4$ for 5 h. After oxidation of the SAM the wafers were rinsed with water and transferred immediately into the deposition medium, an aqueous solution of 4 mM zirconium (IV) sulfate tetrahydrate in 0.4 M hydrochloric acid. The temperature of the deposition medium was ramped slowly (~1 K/min) to 323 K. Films were deposited over time periods of 24–96 h in order to prepare films of various thicknesses to suit the different characterisation techniques employed; thinner films to maximise the conductivity of the samples and thicker to minimise substrate contributions. On removal from the deposition medium the films were rinsed with water and blown dry using argon.

Thermal treatment of the films was performed in argon as a pyrolysis, to avoid potential heat damage to the film from combustion of the SAM, or in synthetic air as a calcination, to mimic the preparation of a typical powder catalyst. The films were heated to 823 K in 125 ml/min of

the chosen atmosphere for 2 h, ramping the temperature up and down at 5 K/min.

2.2. Characterisation

The surface chemical composition of the films was investigated by X-ray photoelectron spectroscopy (PHOIBOS 150 analyser, Specs-GmbH) using Mg Kα excitation (hν = 1256.3 eV) and a pass energy of 30 eV. A Shirley background was subtracted and binding energies were corrected to Zr $3d_{5/2}$ = 182.2 eV of ZrO_2.[39] Atomic sensitivity factors for Zr 3d, O 1s, and S 2s were taken from Ref. [40].

Topographical imaging of the films was performed using a Hitachi S-4100 scanning electron microscope (SEM) with a Thermo Noran System SIX energy dispersive X-ray detector (EDX). The SEM was operated at 5 kV using a working distance of 9 mm for imaging and 15 mm for EDX measurements.

Cross section high resolution transmission electron microscopy (HRTEM) was performed on 24 and 48 h deposited calcined films. The samples were prepared by first cutting the wafers and gluing them together, film surface to film surface, then mechanically polishing and dimpling them down to 5–10 μm, followed by ion milling with a Gatan precision ion polishing system operated at 3.5 kV using Ar^+ ions. To minimise heating of the samples a single unfocused ion beam was used and the samples were rotated. Analysis was performed using a Philips CM200 transmission electron microscope with a field emission gun operated at 200 kV and a Gatan Tridiem imaging filter. Fast Fourier transformation of the images was employed to analyze the structure of small areas or individual grains.

2.3. Adsorption–desorption equilibrium measurements

The sample temperature was measured via a K-type thermocouple inserted into a groove in the silicon support and controlled by liquid N_2 cooling and resistive heating (for isobaric measurements) or electron bombardment (for *in situ* activation), in an apparatus similar to the one described in Ref.[41]. Atmospheric pressure activation was performed in an adjacent chamber with a flow directed across the sample and heating via a lamp positioned in front of the sample. Sample transfer between the two chambers was accomplished under vacuum.

2.3.1. Isobar measurements by XPS

Interaction of both a calcined sulfated zirconia thin film and a silicon oxide layer (generated through oxidation of a cleaned silicon wafer in “piranha” solution) with *n*-butane was investigated using Al Kα excitation (hν = 1486.7 eV) XPS, with a pass energy of 50 eV. Binding energies of the sulfated zirconia thin films were corrected to Zr $3d_{5/2}$ = 182.2 eV of ZrO_2,[39] and of the silicon oxide layer were corrected to the elemental silicon component Si 2p = 99.7 eV of Si (100),[39] to account for temperature-induced shifts. Shirley backgrounds were subtracted from all peaks except for the C 1s, for which a linear background was used.

Initial measurements were performed on a calcined sulfated zirconia film and a silicon oxide layer, both activated at 623 K in UHV with a temperature ramp of 20 K/min. Spectra of the UHV-activated samples were recorded in A-D equilibrium, from room temperature to 100 K and back to room temperature. Experiments were carried out under *n*-butane pressures of $2.2x10^{-8}$ and $2.2x10^{-7}$ hPa sequentially.

In order to determine the signal intensity of an "infinitely" thick carbon layer the sulfated zirconia thin film was also exposed to $1x10^{-6}$ hPa *n*-butane at 100 K until the signals originating from the sulfated zirconia film (Zr 3d, O 1s and S 2p) were no longer detectable.

A "blind" isobar experiment without X-ray irradiation during *n*-butane exposure was performed on the silicon oxide layer, to investigate the effects of irradiation. The wafer was exposed to $2.2x10^{-7}$ hPa *n*-butane from room temperature to 100 K. XPS of the O 1s, C 1s and Si 2p regions were recorded prior to and immediately after the adsorption experiment at room temperature in ultrahigh vacuum.

Detailed isobaric measurements were performed on a calcined sulfated zirconia thin film and a silicon oxide layer, while decreasing the temperature only. Activation of the sulfated zirconia thin film was performed at atmospheric pressure in a flow of 40 ml/min synthetic air at 573 K for 30 min (temperature ramp ~20 K/min). The air-activated sulfated zirconia thin film was exposed to $2.2x10^{-8}$ hPa *n*-butane at temperatures from 200 K to 100 K. At 120 K the temperature was held constant for 40 min. The silicon oxide layer, which had been used previously for an adsorption experiment, was reactivated at 623 K in $1x10^{-7}$ hPa O_2 for 1 h, using a temperature ramp of ~20 K/min. The silicon oxide layer was then exposed to $2.2x10^{-8}$ hPa *n*-butane while cooling from 200 K to 120 K.

C 1s Difference spectra, corresponding to the adsorbate signal, were obtained by subtracting the "clean" surface spectrum under UHV prior to *n*-butane exposure from the spectra taken in A-D equilibrium. The area of the difference signal could be converted into a coverage-dependent value using the Lambert–Beer absorption law. Coverage θ is defined as the number of adsorbed molecules divided by the total number of adsorption sites on the adsorbent:

$$\theta \propto \frac{d}{l_e} = -\ln\left(1 - \frac{I_{ads}}{I_{0,ads}}\right)$$

where d is the adsorbate thickness (averaged over the whole surface), l_e is the electron escape depth, I_{ads} is the intensity of the adsorbate signal and $I_{0,ads}$ is the intensity of the signal of an infinitely thick adsorbate layer. Hence, d/l_e is proportional to the adsorbate coverage. The escape depth is given by $l_e = \lambda_e \cos \alpha$, where λ_e is the electron mean free path and α the mean escape angle normal to the surface (for the configuration used α=0°, therefore $l_e = \lambda_e$). λ_e depends strongly on the kinetic energy of the electrons and, albeit to a lesser degree, on the material the electrons are passing through. Reported values of λ_e (for various kinetic energies and materials)[39] can be used to estimate the adsorbate thickness, although wide error margins are to be expected as a result of the uncertainty in λ_e, and the calculated values only have real meaning for full layer coverages. Calculated values are therefore quoted as equivalent adsorbate thicknesses.

2.3.2. Isobar measurements by UPS

He II (hν = 40.8 eV) UPS was also used to investigate the interaction of *n*-butane with calcined sulfated zirconia thin films and silicon oxide layers. Measurements were performed with a pass energy of 15 eV and a -5 V sample bias. Secondary electron curves and He II satellite-induced emissions were not subtracted from the UP spectra presented. Both binding energy and vacuum level (E_{vac}) aligned x-axis scales are given for all UP spectra (which differ by the work function of the spectrometer, 4.6 eV). Sample charging was not evaluated.

Initial measurements were performed on a silicon oxide layer. Spectra were measured in A–D equilibrium at $1x10^{-6}$ hPa while decreasing the temperature from room temperature to 105 K, followed by holding the temperature constant at 105 K for 1 h. In a subsequent experiment, the silicon oxide layer was cooled to 108 K and XP spectra of the surface were taken. The sample was then exposed to $1x10^{-6}$ hPa *n*-butane and the change in signal followed by UPS. After 20 min XP spectra of the surface were taken with a low resolution to minimise beam damage.

Detailed measurements were performed on fresh samples activated at 573 K under atmospheric pressure in a flow of 40 ml/min synthetic air for 30 min, using temperature ramps of ~20 K/min. Spectra were measured in A-D equilibrium under constant *n*-butane pressures of $1x10^{-8}$, $1x10^{-7}$ and $1x10^{-6}$ hPa at temperatures from room temperature to ~110 K, sequentially. After each isobar the sample was moved out of the UV beam, the chamber was evacuated, and the sample was heated resistively up to room temperature. Before and after the sets of isobars, XPS measurements of samples were performed in UHV.

After the set of isobars, the sulfated zirconia thin film was reactivated under the same conditions as were used for the original activation. The film was then exposed to $1x10^{-6}$ hPa *n*-butane at temperatures down to 100 K while turned out of the irradiating beam (a non-irradiated isobar). UP and XP spectra were recorded in UHV at room temperature prior to and after performing the non-irradiated isobar. The sulfated zirconia thin film was again reactivated and exposed to $1x10^{-6}$ hPa *n*-butane for 3 h at room temperature under He II UV irradiation. UP spectra were recorded after each hour and XP spectra of the sample were measured in UHV before and after the 3 h *n*-butane exposure.

To obtain adsorbate spectra, the data series recorded of the silicon oxide layer and the sulfated zirconia thin film in A–D equilibrium were analysed as outlined in Ref. [30] The clean spectrum obtained prior to performing the isobar was subtracted from the spectra taken under *n*-butane A–D equilibrium conditions, after applying an attenuation factor to the clean spectrum and shifting the energy scale of the spectra acquired under *n*-butane A–D equilibrium. The alignment shift and attenuation factor are applied such that there is not an increase in the difference spectra between binding energies of ~2.5–4.0 eV (where no spectral contributions from the adsorbate are expected). Misalignment of the spectra can result in the introduction of artificial structures; alignment shifts and attenuation factors were varied until such artefacts were minimised.

The attenuation of the clean spectrum can be converted into a coverage-related value using the Lambert–Beer absorption law:

$$\theta \propto \frac{d}{l_e} = -\ln\left(\frac{I_{sub}}{I_{0,sub}}\right)$$

where I_{sub} is the substrate (adsorbent) intensity and $I_{0,sub}$ is the substrate intensity prior to adsorption. Thus, $(I_{sub}/I_{0,sub})$ is the attenuation factor used to form the difference spectra. The carbon layer thickness was estimated in a similar way for the XPS measurements of the silicon oxide layer after exposure to $1x10^{-6}$ hPa *n*-butane for 20 min at 108 K, using the attenuation of the Si 2p peak.

Isosteric heats of adsorption were derived for *n*-butane on the calcined sulfated zirconia thin film from the sets of isobars generated at the different pressures using the Clausius–Clapeyron equation.[30] For a given coverage, the gradient of ln *p* plotted against 1/T is equivalent to the isosteric heat of adsorption over the gas constant, R.

3. Results

3.1. Thermal treatment experiments

XPS measurements of the as deposited films show that signals from the silicon substrate decrease with increasing deposition time. Two maxima of the Si 2p are detected, one at a binding energy of Si $2p_{3/2}$ = 99.7 eV consistent with Si(100) and the other at a binding energy of Si $2p_{(3/2+1/2)}$ = 103.7 eV, in accordance with oxidised silicon.[39]. Signals arising from the zirconia film are

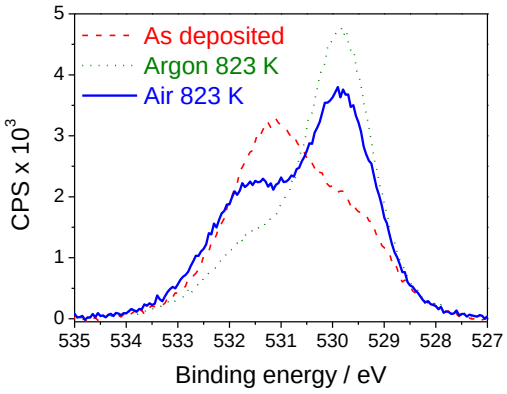

Fig. 1: O 1s XP spectra of films deposited over 48 h as deposited and after argon or air treatment at 823 K.

shifted towards higher binding energies because of charging, an offset of around 2.2 eV is observed. After correction of the binding energies, the maximum of the S 2p (S $2p_{3/2+1/2}$) signal is detected at a binding energy of 168.4 eV, indicating a sulfur oxidation state of +6. The O 1s signal (Figure 1) is composed of at least two peaks, the lower binding energy peak at around 529.4 eV relates to oxide anions and the higher binding energy peak at ca. 531.1 eV corresponds to sulfated and hydroxide species. Assuming the charging correction is also valid for the carbon signal, the C 1s peak has a maximum at ~284.0 eV, which is similar to the reported value of "chain" carbon[42] as would be expected from the SAM.

XP spectra of the films after the two different thermal treatments show the loss of sulfur, as is apparent from the relative intensity of the S 2p as well as the S 2s region in the spectra, and from the shape of the O 1s signal (Figure 1). The higher binding energy component of the O 1s signal (relating to hydroxyl and sulfate groups) is reduced after both thermal treatments, but more significantly for the treatment in argon. After thermal treatment of the films in argon no sulfur is detectable in the S 2p or S 2s regions. Thermal treatment of the films in synthetic air retards the loss of sulfur and thus elemental compositions of the films are comparable to a typical active powder catalyst (Table 1).[43] In addition to the loss of sulfur, the C 1s signal is diminished and shifts to 284.6 eV, consistent with the decomposition of the SAM and the main source of carbon being either atmospheric contamination (adventitious) or SAM decomposition products. The silicon substrate peaks are more prominent after thermal treatment, indicating a decrease in layer thickness. Estimation of the thickness of the air-treated films from the intensity of the Si 2p signal (using an electron mean free path of 3.2 nm, calculated from Ref. [44]) yields values of 2–12 nm, increasing linearly with deposition time (see Figure 2).

SEM images (not shown) reveal the surfaces of the as deposited and thermally treated films to all be mainly

Table 1: Elemental compositions calculated from XPS data of as deposited and thermally treated films deposited over 48 h. Samples compared to a typical active tetragonal powder sulfated zirconia sample.[43] n.d. = not detected

Atomic %	Zr	O	S
As deposited	18.6	73.5	7.9
Argon 823 K	30.0	70.0	n.d.
Air 823 K	25.8	71.1	3.2
Calcined powder	27	68	5

smooth, homogeneous and crack free. However, some spherically shaped particles with diameters up to 2 μm are observed on the as deposited film surface. These particles appear to remain unchanged, as does the film surrounding them, after the two different thermal treatments. EDX analyses reveal that the as deposited film and particles consist of zirconium, oxygen and sulfur. After thermal treatment EDX analyses of the films overall elemental compositions results in similar values to those from XPS measurements; no sulfur was detected in the argon-treated film and a slightly lower sulfur content compared to the as deposited film for the air-treated film. Focusing of the incident electron beam for EDX analysis on the particles shows that their compositions differ from that of the film for the argon-treated sample, in that they contain sulfur. However, the composition of the particles on the air-treated films is similar to the film composition. Elemental compositions of surface and particles of the air-treated films by EDX analysis are comparable to a typical powder catalyst.

Cross sectional HRTEM images of air-treated films deposited over 24 and 48 hours are shown in Figure 3a and b. TEM analyses reveal both films to be continuous, with average thicknesses of 2.5 (24 h deposition) and 5.5 nm (48 h deposition). The film thickness of the 24 h deposited film varies from 1 to 5 nm. The 48 h film is, however, of relatively homogeneous thicknesses (within 1 nm). HRTEM images show the 24 h film to be mainly amorphous with some crystals in the thicker areas of the film; crystals with sizes between 1–10 nm parallel to the film are detected. The 48 h film is shown to be fully crystalline with crystal

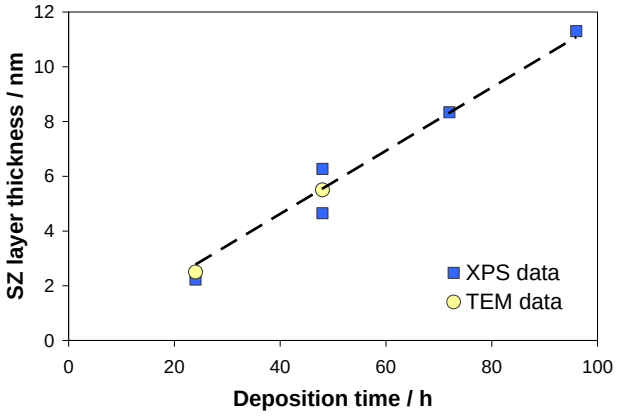

Fig. 2: Air-treated sulfated zirconia film thickness after various deposition times calculated from XPS and TEM results.

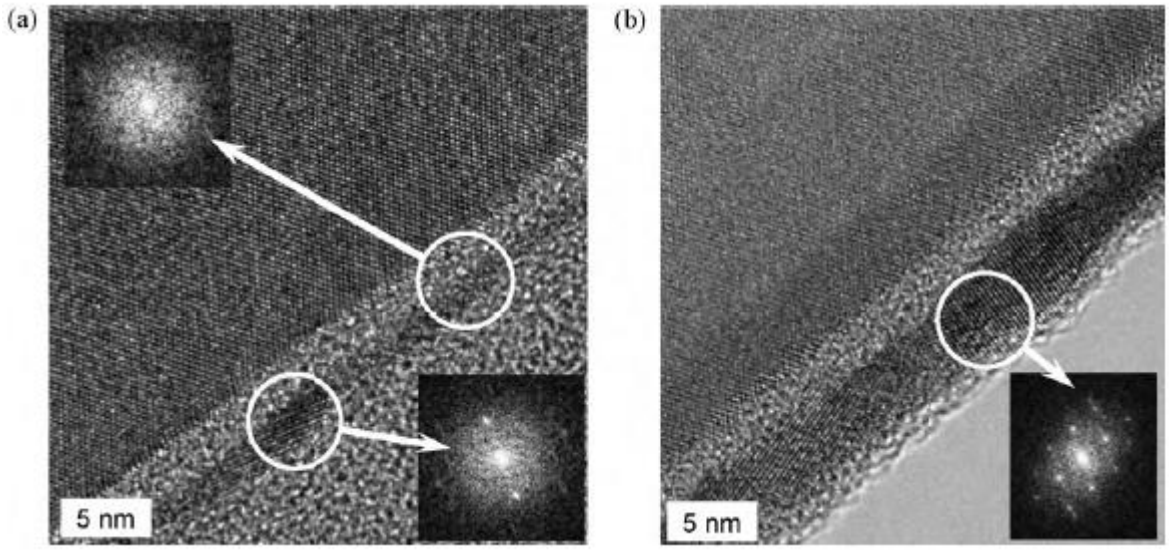

Fig. 3: HRTEM cross section images (and Fourier transforms of selected areas inset) of calcined sulfated zirconia thin films after (a) 24 h and (b) 48 h depositions. Top left to bottom right sequence shows the silicon wafer (about half of the image), an about 3 nm thick layer of silicon oxide (light grey) and the sulfated zirconia layer (as a dark band with lattice fringes visible).

sizes from 5 up to 30 nm. Fourier transform analyses of selected areas of the HRTEM images (inset Figure 3a and b) reveal the structures of the crystalline layers from both films to be consistent with the tetragonal phase. Minor amounts of the cubic phase cannot be excluded; however, no monoclinic phase was present in the areas of the films examined.

3.2. Adsorption–desorption equilibrium measurements

3.2.1. Isobar measurements by XPS

C 1s XP difference spectra of the sulfated zirconia thin film at an *n*-butane pressure of 10^{-7} hPa (initial measurements) are shown in Figure 4a. An increase in the C 1s signal intensity is seen upon decreasing the temperature below ~140 K, concomitantly the substrate peaks (O 1s and Zr 3d, not shown) decrease in intensity, consistent with the adsorption of *n*-butane. Increasing the sample temperature from 100 K back to room temperature and evacuation results in a decrease of the C 1s signal; however, a significant fraction of the signal remains (approximately 35% of the signal at 100 K). Repeating this experiment with a silicon oxide layer also results in the adsorption of *n*-butane at low temperatures and the formation of a carbonaceous species that remains after evacuation.

The initial isobars on both the sulfated zirconia thin film and the silicon oxide layer performed at an *n*-butane pressure of 10^{-8} hPa also show the formation of carbonaceous deposits that remain after evacuation. The total adsorbate coverage on the samples during the isobars at 10^{-8} hPa is much lower than during the isobars at 10^{-7} hPa (by roughly a factor of 2), as is the fraction that is irreversibly adsorbed (~10%).

A "blind" isobaric experiment on the silicon oxide layer, without irradiating during *n*-butane exposure (at 2.2×10^{-7} hPa and including cooling to 100 K and reheating to room temperature), does not lead to a significant increase in the carbon signal. Thus, carbon deposits that are not removed after evacuation are attributed to decomposition of the adsorbate by irradiation and are hereafter referred to as beam damage residues. The amount of beam damage residue formed is proportional to both the adsorbate coverage and irradiation time.

Isobars derived from detailed XPS measurements are shown in Figure 4b. These measurements were performed while decreasing the temperature only on freshly activated samples at low *n*-butane pressures (10^{-8} hPa) in order to minimise beam damage residues. Measurements of the air-activated sulfated zirconia film at a constant temperature (120 K) during butane exposure do not show a significant increase in adsorbate coverage with time (in comparison to changes with temperature), thus the fraction of adsorbate coverage that is beam damaged during the measurement is considered negligible. Adsorption on the sulfated zirconia thin film at an *n*-butane pressure of 10^{-8} hPa is initially detected at ~150 K and significantly increases below 120 K. The adsorbate coverage on a sulfated zirconia thin film is clearly higher than for the silicon oxide layer under the same conditions between 150−120 K.

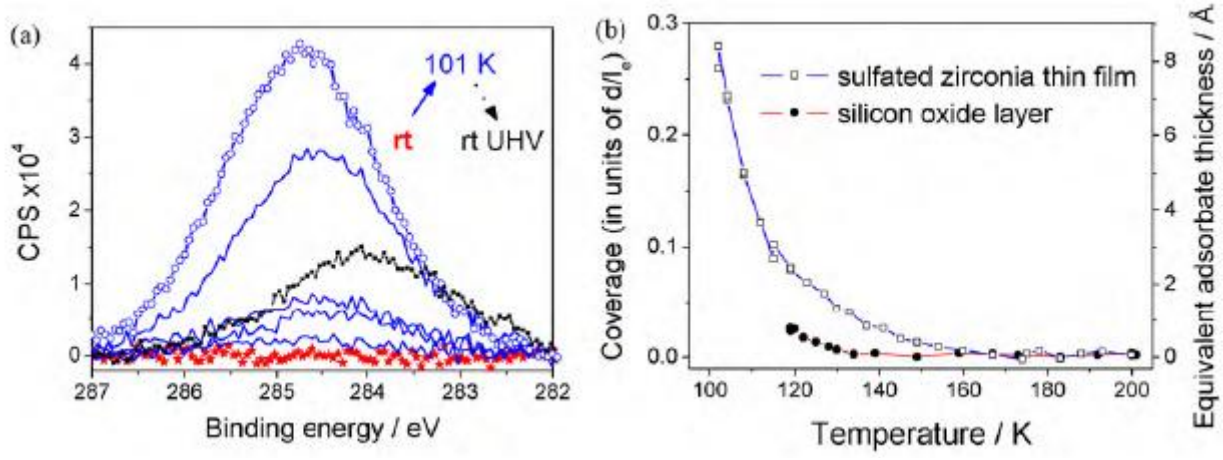

Fig. 4: (a) C 1s XP difference spectra of a sulfated zirconia thin film under A-D equilibrium of $2.2x10^{-7}$ hPa *n*-butane measured while decreasing temperature from room temperature (solid stars) to 101 K (solid lines: intermediate temperatures, open circles: 101 K) and after increasing temperature to room temperature and evacuation (solid squares). Spectrum of clean (as introduced) specimen subtracted.
(b) $2.2x10^{-8}$ hPa *n*-Butane isobars on a sulfated zirconia thin film and a silicon oxide layer.

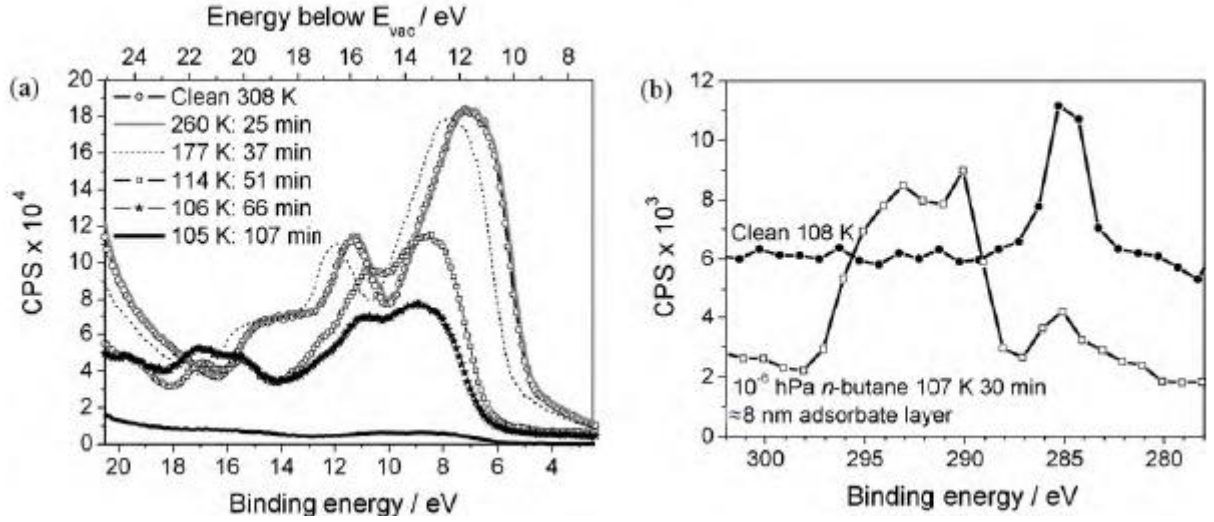

Fig. 5: (a) UP Spectra of a silicon oxide layer as introduced (clean) at room temperature under UHV and under $1x10^{-6}$ hPa *n*-butane A–D equilibrium conditions from room temperature to 105 K, time exposed to *n*-butane given in minutes. (b) C 1s XP Spectra of "clean" silicon oxide layer at 108 K under UHV and after 30 minutes exposure to $1x10^{-6}$ hPa *n*-butane.

3.2.2. Isobar measurements by UPS

UP spectra of a silicon oxide layer under UHV conditions (clean) and at an *n*-butane pressure of $1x10^{-6}$ hPa (initial measurement) are shown in Figure 5a. As the temperature is decreased all signals shift to higher binding energies, which may be caused by band bending[45] at the silicon-oxide interface, photovoltaic effects[46,47] and possibly also variations in charging of the oxide overlayer. The presence of an adsorbate can affect the work function and thus also result in binding energy shifts.[30] Upon cooling, the shape of the spectra changes indicating adsorption of *n*-butane. A decrease in overall signal intensity during adsorption is observed, evidently from the adsorbate having a lower photoelectron cross section than the adsorbent.

At low temperatures (below 110 K) the signal intensity across the entire measured region (as shown in Figure 5a) significantly reduces in intensity with time. Comparison of XP spectra (with short acquisition time to minimise beam damage) of the silicon oxide layer at 108 K in UHV and after exposure to $1x10^{-6}$ hPa for 20 minutes shows the deposition of carbon species with binding energies up to 10 eV higher than the initial carbon signal (Figure 5b). C 1s binding energies of above 292 eV are only possible from carbon bonded to fluorine,[39] which is not present (as shown by XPS). Therefore, the shift must arise from strong charging of the thick adsorbate layer, which is obviously insulating. The valence orbitals of the charged adsorbate are shifted so far towards higher binding energies in the UP spectrum that they disappear from the measured range and

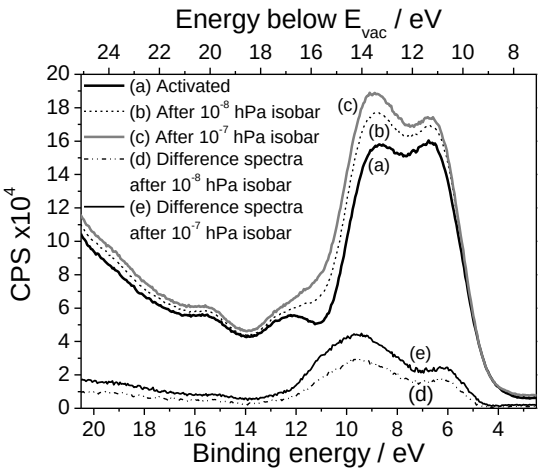

Fig. 6: UP spectra of sulfated zirconia thin film after activation and sequential 10^{-8}, and 10^{-7} hPa *n*-butane isobars. Difference spectra indicating the beam damage residues formed after the 10^{-8} and 10^{-7} hPa *n*-butane isobars are also shown.

are indistinguishable from the secondary electron curve. Only a minor contribution from the uncharged adsorbate is still observed.

UP spectra of the samples taken in UHV before and after each of the detailed isobar measurements show the build-up of deposits that are not removed by evacuation (Figure 6). Such deposits form on the silicon oxide layer and the sulfated zirconia thin film and their amount increases with increasing pressure during the isobaric measurement (up to a thickness corresponding to $d/l_e \approx 0.05$). These deposits detected by UPS are, however, below the XPS limits of detection.

Regeneration of the sulfated zirconia thin film after the set of three isobars results in the removal of the majority of species remaining after evacuation. Exposing the regenerated sulfated zirconia to $1x10^{-6}$ hPa *n*-butane at 100 K without irradiation or for 3 h at room temperature irradiating with He II radiation does not result in changes to the shape of the valence band spectra. Therefore, the deposited species remaining after the isobaric measurements are beam damage residues and UV irradiation of the sample in *n*-butane at room temperature does not induce adsorption.

To limit the effect of the beam damage residues, the spectrum obtained (in UHV) immediately prior to each isobar is subtracted from the spectra obtained in A–D equilibrium to produce the difference spectra. Difference spectra (from both materials studied) generated for measurements performed under *n*-butane A–D equilibrium show the development of spectral features that resemble those of gaseous *n*-butane[48] but are significantly broadened. Adsorption is observed at higher temperatures than during the XPS measurements, probably because of the higher surface sensitivity of UPS.

The sulfated zirconia difference spectra recorded at an *n*-butane pressure of 10^{-6} hPa and at various temperatures are shown in Figure 7b; similar spectral changes are

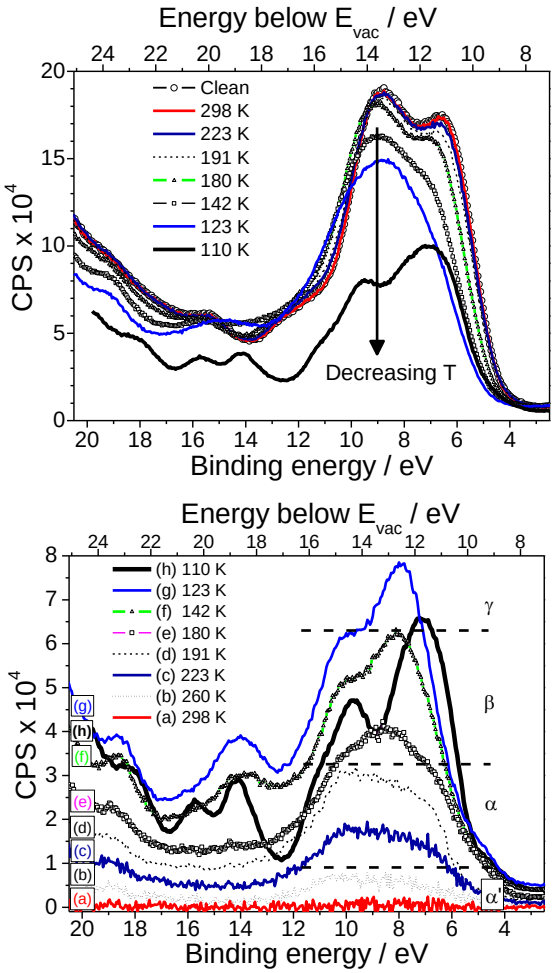

Fig. 7: UP spectra of a sulfated zirconia thin film during A–D equilibrium at $1x10^{-6}$ hPa *n*-butane: (a) raw data with "clean" UHV spectrum and (b) "clean" subtracted adsorbate difference spectra.

observed for the difference spectra obtained at *n*-butane pressures of 10^{-8} and 10^{-7} hPa. At low coverages ($d/l_e < 0.3$, labelled region α) the spectral features are significantly perturbed compared with the gas phase spectrum[48], indicating a strong interaction between *n*-butane and surface. Above a certain coverage ($0.3 < d/l_e < \sim1$, labelled region β) the development of features that resemble the gaseous spectrum of *n*-butane[48] become apparent, suggesting a low level of perturbation and hence a weak interaction. At high coverages ($d/l_e > \sim1$, labelled region γ) the overall intensity of the spectra decreases, because of charging of the adsorbate as indicated by XPS measurements. A step in the isobars generated from the attenuation of the adsorbent indicate the α region can be further split into two different states, labelled α' for low coverages ($d/l_e < 0.05$) and α for higher coverages ($0.05 < d/l_e < 0.3$) in Figures 7b and 8b.

Heats of adsorption (Figure 9) calculated from the isobars decrease initially from 69 to 41 kJ/mol with increasing coverage in the α' region; they then increase to ~47 kJ/mol and decrease again to 34 kJ/mol with increasing coverage in the α region. Values of ~28 kJ/mol, independent of coverage, are obtained in the β region.

a)

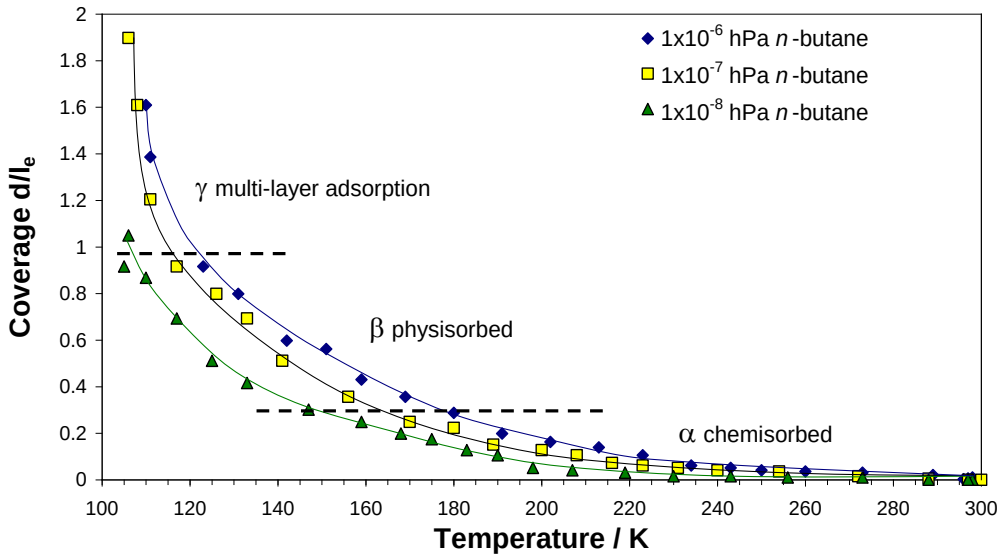

b)

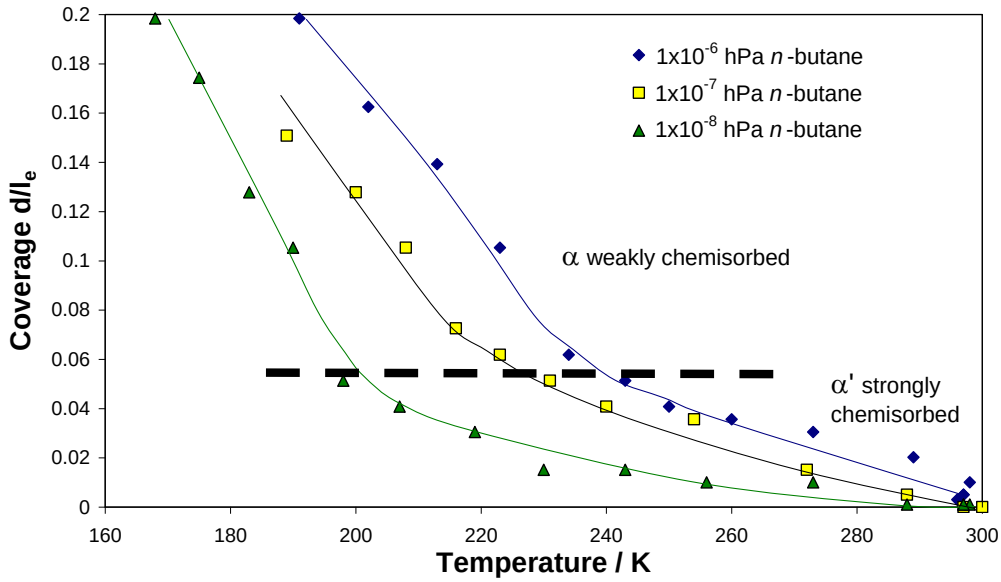

Fig. 8: Isobars derived form A–D equilibrium UPS measurements on a sulfated zirconia thin film, (a) complete isobars and (b) initial coverages only

4. Discussion

4.1. Validation of thin films as model

The sulfated zirconia films were characterised by a variety of methods to ensure that they are representative models of a typical powder catalyst and are suitable for surface science investigations. Topographical studies by SEM showed the surfaces of the as deposited and thermally treated sulfated zirconia films to be largely free of adhering particles and smooth. No influence of the particles was detected using XPS, for example no differential charging was observed, which would obfuscate the results.

Thermal treatment of the films in argon results in an almost complete loss of sulfur whereas after thermal treatment in air the majority of sulfate is retained. Decomposition reportedly yields SO_2 (g) + ½ O_2 (g)[49] and, consequently, this pathway is suppressed in air. Therefore, films thermally treated in air were used for further investigations. The elemental composition of both the films and particles adhering to the films, after thermal treatment in synthetic air, were shown to be equivalent and similar to an active powder sample.

Structural investigations of the air-treated films by TEM show that very thin films do not crystallise. In order to form a fully crystalline material a film thickness of at least ~5 nm is required. Films that were deposited over 48 h

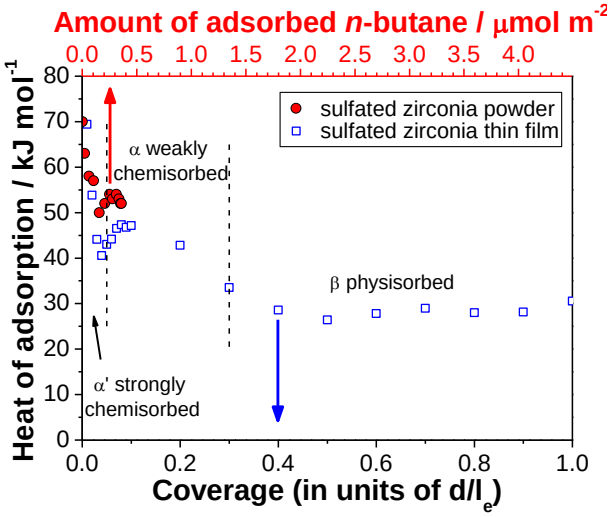

n-Butane heats of adsorption on a sulfated zirconia thin film (from isobaric measurements) and on a sulfated zirconia powder (from microcalorimetric measurements).[69] Amount of *n*-butane adsorbed on the sulfated zirconia powder is aligned to the *n*-butane coverage of the sulfated zirconia thin film assuming a cross sectional area of 33.2 Å² per butane molecule.[62]

were found to consist of tetragonal crystals. The monoclinic phase is the thermodynamically stable phase for extended crystals of zirconia. The tetragonal phase is stabilised by the formation of small crystals (less than 30 nm in size) because of its lower surface energy in comparison with the monoclinic phase[50-53] and by the presence of sulfate.[4] The tendency of very thin films not to form the tetragonal phase may be explained by the surface energy stabilisation of amorphous relative to tetragonal zirconia.[54] Some of the experiments (specifically, measurements of isobars by XPS) were performed with the thin and thus only partially crystallised samples, and the interpretation of these experiments must consider the small tetragonal fraction of the films. The size of the tetragonal crystallites is equivalent to those of active sulfated zirconia powders.[55] In conclusion, the produced films are considered a suitable model for surface science studies.

4.2. Elimination of beam damage and charging problems

XPS measurements after adsorption and desorption of *n*-butane under isobaric conditions indicate that a small fraction of the adsorbate is decomposed in the X-ray beam, resulting in the formation of residues that remain after evacuation. Organic materials are known to be sensitive to beam damage due to their insulating nature and relatively weak bonds.[56] Beam damage of organic materials is believed to be caused by low energy (secondary) electrons,[57] which are formed by the inelastic scattering of photoelectrons in a cascading effect. Experiments performed on fresh samples during decreasing temperature show the effect of beam damage during the measurement to be negligible. Such artefact-free data show that the adsorption of *n*-butane on sulfated zirconia thin films is promoted compared to adsorption on a silicon oxide layer.

To deduce isosteric heats of adsorption, multiple isobars at various pressures need to be performed on the same surface; this could be done in principle by only studying the initial stages of adsorption or reactivating the sample after each isobar. If just the very low coverages were to be studied (which can be considered the catalytically relevant chemisorption states), the amount of beam damage could be considered insignificant. However, in practice, differentiating between the interesting adsorbate coverages and levels at which beam damage becomes significant during an experiment is very difficult. Reactivating of the samples after each isobar to remove the beam damage residues may result in changing surface chemistry (for example OH coverage). In order to perform multiple isobars on the same surfaces UPS was used instead of XPS to avoid beam damage. Significantly fewer low energy secondary electrons are expected from the inelastic scattering of photoelectrons from He II UV radiation than Al Kα X-ray radiation because of the lower photon energy (48.8 eV vs. 1486.7 eV).

Measuring the adsorbate coverage during *n*-butane A–D equilibrium using UPS drastically reduces the amount of beam damage residue compared to XPS (to below the XPS detection limit). However, beam damage residues are still seen by UPS. In order to reduce adsorbate irradiation (and hence limit beam damage effects) UPS isobars were performed only while decreasing the sample temperature, the sample was turned out of the beam while the temperature was increased and subsequent isobars were performed at higher pressures.

UP spectra of the beam damage residues (Figure 6) are similar to graphitic species.[36] The high signal intensity of such species and the marginal attenuation of the adsorbent spectrum indicate that the residues probably form 3-dimensional islands. Since the reported heats of adsorption of *n*-butane on graphitic materials (32.6–33.9 kJ/mol)[58-60] are much lower than those for adsorption on sulfated zirconia[61] and the shape of the difference spectra generated does not change with increasing pressure of the isobaric measurements (and hence also the amount of beam damage residues), it is assumed that at low coverages (during chemisorption) adsorption occurs on the sulfated zirconia film and not on the beam damage residues. Saturation coverages of the various adsorption sites, as indicated by changes in the UP spectra and isobar gradients, are not influenced by the increase of the beam damage residues in consecutive measurements. The reduction in surface area of the sulfated zirconia film by beam damage residues is thus considered negligible.

UP spectra recorded at low temperatures and thus high coverages show a significantly reduced intensity in the measured region (Figure 7a), which can only be interpreted by assuming a highly charged adsorbate state with a photo

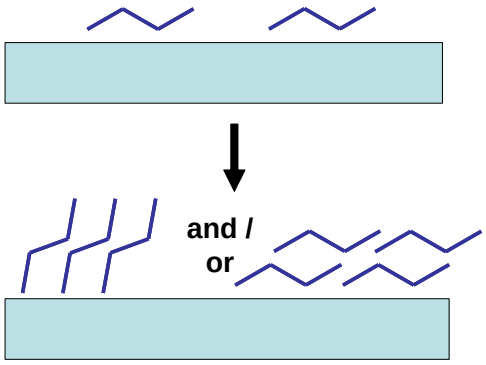

Fig. 10: Proposed adsorbate structure changes with increasing coverage.

electron signal that overlaps with the secondary electron peak. XPS measurements of the *n*-butane-exposed, silicon oxide layer, after the UPS signal is significantly reduced, reveal the adsorbate coverage to be in excess of a typical monolayer (when a monolayer is defined as the complete occupancy by the adsorbate of all adsorbent adsorption sites). Thus a multilayered adsorbate structure must exist. However, the change in the shape of the spectra at very low temperatures indicates that the adsorption geometry of the initial adsorption states may change as well. These possibilities are illustrated in Figure 10. The charging adsorbate state was not seen during isobar measurements by XPS, thus it may have been decomposed by X-ray irradiation. The charging adsorbate state was not further investigated because it was only observed at high coverages, that is, during multilayer adsorption and therefore it does not reflect adsorption on catalytically active sites. Detailed UPS A–D equilibrium measurements were therefore discontinued when a significant decrease in signal intensity was observed.

4.3. Interpretation of isobars

Analysis of the isobars obtained through XPS measurements showed that the adsorption of *n*-butane on sulfated zirconia is promoted relative to adsorption on silicon oxide. Difference spectra generated from UPS measurements on the sulfated zirconia thin film indicate that at lower coverages the adsorbate interacts more strongly with the adsorbent than at higher coverages; this trend is evident from both the shape of the valence orbitals (observed between binding energies of 5–12 eV) in comparison with the *n*-butane gaseous spectrum,[48] and from the relatively higher binding energies (Figure 7b). Three of the four C 2s orbitals of adsorbed *n*-butane are observed between binding energies of 13–20 eV, the fourth orbital is assumed to be hidden by the secondary electron curve. The spectral features of the adsorbate, when aligned to the vacuum level energy, are shifted by approximately 0.4 eV with respect to the gas phase *n*-butane spectrum[48] because of the relaxation effect (although, as the sulfated zirconia thin film and hence also the adsorbate may be charging, the absolute relaxation shift could be larger than the value given here).

The mean free path of the photoelectrons during the UPS measurements is approximately 0.5 nm,[44] which is similar to the thickness of a complete *n*-butane monolayer coverage reported on various surfaces {0.41 nm on MgO (100)[62] and Ag (111)[63] }. The saturation of the β state, which occurs at $d/l_e \approx 1$, thus corresponds to the completion of a monolayer. Surface sites on the sulfated zirconia thin film lead to three different adsorption states of *n*-butane, which distribute approximately to 5% region α', 25% region α and 70% region β. Considering the heats of adsorption and spectral features, the adsorption states α', α and β are attributed to strong chemisorption, weak chemisorption and physisorption, respectively. The region γ is attributed to multilayer adsorption. The second and subsequent layers may not necessarily be considered as condensation, as such a state has been reported to occur only after 2.5 monolayers for butane on multiwalled carbon nanotubes (which have lower initial heats of adsorption than sulfated zirconia).[64]

4.4. Evaluation of isosteric heats of n-butane adsorption

Initial *n*-butane heats of adsorption of ~59 kJ/mol obtained on the sulfated zirconia thin film and the general trend of the heats to decrease with increasing coverage are in good agreement with previously reported results on sulfated zirconia powders (50–60 kJ/mol).[61,65-68] An increase in the heats of adsorption with increasing *n*-butane coverage, as seen in the α region on the sulfated zirconia thin films (shown in Figure 9), has also been observed during microcalorimetric measurements on some powder sulfated zirconia materials.[69] Such an increase may be the result of adsorbate–adsorbate interactions, which would indicate the alkane molecules are situated next to one another. Adjacent surface sites would allow the skeletal isomerisation to proceed via a bimolecular surface reaction between two adsorbed species, as proposed by Fogash et al.[70] on the basis of a kinetics investigation.

To compare the heats of *n*-butane adsorption on the sulfated zirconia thin film with those obtained on powders, the coverage has to be converted to mol/g or mol/m^2. Assuming an *n*-butane cross sectional area of 33.2 Å^2, as determined for a monolayer coverage of *n*-butane on MgO,[62] a monolayer of *n*-butane corresponds to a total of 3.0×10^{18} molecules/m^2. Therefore, the 5 and 25% monolayer coverage adsorption regions α' and α equate to *n*-butane surface densities of approximately 1.5×10^{17} and 7.5×10^{17} molecules/m^2 respectively, or a total of 0.9×10^{18} molecules/m^2.

Aligning the amount of *n*-butane dosed onto a sulfated zirconia powder[69] with the *n*-butane coverage on the sulfated zirconia film in Figure 9 reveals the onset of increase in adsorption heats to occur at approximately the same loadings on both specimens. The heats of adsorption

in the α region of the sulfated zirconia thin film are slightly lower than those of the presented powder material (~47 kJ/mol versus 52–54 kJ/mol), however they are within the range of reported values on powders at higher coverages (45 kJ/mol[65] for 0.20 μmol/m², 38 kJ/mol[66] for 0.36 μmol/m² and 40 kJ/mol[68] for 0.55 μmol/m²).

4.5. Adsorption sites

To identify the nature of the adsorption sites, the coverage of the zirconia with sulfate groups needs to be estimated. XPS measurements show that the Zr:S atomic ratio (based on the Zr 3d and S 2p peak areas and reported atomic sensitivity factors[40]) of the activated sulfated zirconia thin film is 5.4. Assuming a homogeneous distribution of sulfur and zirconium within the thin film over the XPS measurement depth, a sulfate surface area of 31 Å²[71] and a zirconia surface 2 x 2 unit cell of 6.425 x 7.284 Å,[8] the sulfate groups are shown to cover ~33% of the surface, which is equivalent to a surface site density of ~1.1×10^{18} S atoms/m². Alternatively assuming the sulfate groups are situated on the surface of zirconia crystals, a layer model that accounts for attenuation of the zirconium signal can be used to estimate the sulfate surface density. Such a model results in the calculated thickness of the sulfate layer being in excess of a monolayer coverage, which is not considered viable given the preparation route of the zirconia thin films and the fact that polymeric sulfates (higher than disulfates) were not observed by theoretical studies.[8]

Previously reported IR studies indicate the adsorption of *n*-butane to occur on hydroxyl groups on sulfated zirconia.[73] Furthermore, XPS investigations on the interaction of sulfated zirconia thin films with *n*-butane under reactive conditions[74] show the attenuation of the zirconium signal to be greater than sulfur upon carbon deposition, which suggests adsorption on zirconia rather than coverage of the sulfate groups. However, given the similar coverages and densities of the chemisorbed *n*-butane (α' and α together account for 30% of the surface sites) and sulfate surface sites (33% percent coverage), chemisorption of *n*-butane is proposed to occur in close proximity of the surface sulfate species. As the surface areas (and hence structures) of both sulfate and *n*-butane molecules are assumed (based on literature values) the correlations between the activated sulfate and total chemisorbed butane surface coverages or densities are surprisingly good. It is thus proposed that the strong chemisorption sites arise from the presence of a minority, active, disulfate species.[8,9] Hence the weaker, more dominant chemisorption sites are ascribed to mono-sulfate species. The range of *n*-butane heats of adsorption for both the disulfate and mono-sulfate species are attributed to there being a distribution of similar adsorption sites. It is thus envisioned that the chemical environment of the disulfate and mono-sulfate species, for instance hydroxyl groups or defects, play a key role for the adsorption properties of the sites. In other words, the sites can be considered ensembles of sulfate groups and their surrounding.

5. Conclusions

To study the surface chemistry of sulfated zirconia, thin films containing zirconium, oxygen and sulfur were synthesised using a biomimetic route. The thickness of the films was found to play a crucial role in the formation of the tetragonal phase; if the films are too thin the layer will not crystallise during thermal treatment. Calcined films were found to have the essential features, including equivalent sulfur content and crystalline phase, of active powder catalysts,[43] thus validating them as a model system. These films enable surface science techniques to be applied while not compromising the chemical complexity of the catalyst. Different types of adsorption sites on sulfated zirconia could thus be identified and quantified, with more detail than was previously possible.

The adsorption of *n*-butane on sulfated zirconia thin films under adsorption–desorption equilibrium conditions was detected by XPS and UPS. XPS measurements under isobaric conditions showed the sulfated zirconia thin films to promote the adsorption of *n*-butane as compared to a catalytically inactive material (a silicon oxide layer).

UPS measurements under isobaric conditions detected two distinctly different chemisorption sites for *n*-butane on sulfated zirconia. Adsorption of *n*-butane equivalent to 0–5 and to 5–25% of a monolayer on the sulfated zirconia thin films, releasing heats of between 59–40 and 47–34 kJ/mol, is ascribed to strong and weak chemisorption, respectively. The sites are considered to be ensembles characterised by disulfate and mono-sulfate species, respectively. Variations in the chemisorption heats are ascribed to a diverse chemical environment of the sulfate species. An increase in adsorption heat with increasing coverage was observed at ~5–8% of a monolayer, this trend is believed to result from adsorbate–adsorbate interactions. Sites in close proximity to one another would allow for isomerisation proceeding via a bimolecular surface reaction. Physisorption on the films generates heats of ~28 kJ/mol, for coverages between 30% up to a complete monolayer. The deduced heats of adsorptions are in good agreement with values obtained from powder sulfated zirconias,[65-68] indicating that the nature of the sites on powder materials can be identified with the help of the assignments made by use of model thin films .

Acknowledgements

The authors would like to thank Prof. F. Aldinger's department at the Max Planck Institute for Metals Research, Stuttgart, for the surfactant, Wacker Siltronic AG for the silicon wafers (100, p-type), A. Klein-Hoffmann for preparing cross sections of the thin films, G. Weinberg for

performing the SEM and EDX measurements, and Dr. S. Wrabetz for discussion of and providing the powder calorimetry data.

Project funding from the DFG priory program (SPP) 1091 ‘‘Bridging the Pressure and Material Gap in Heterogeneous Catalysis’’, individual project Je 267/1, is gratefully acknowledged. Discussions and input from the fellow members of this priory program; Prof. H. Papp and Dr. C. Breitkopf from the Universität Leipzig; Prof. J. A. Lercher, Dr. R. Olindo and X. Li from the Technische Universität München; Prof. W. Widdra, Dr. K. Meinel and Dr. K.-M. Schindler from the Martin-Luther-University Halle-Wittenberg; Prof. J. Sauer and Dr. A. Hofmann from the Humboldt-Universität zu Berlin; are highly appreciated. Personal financial support for R.L. from the International Max Planck Research School is also gratefully acknowledged.

References

[1] V. C. F. Holm and G. C. Bailey, US Pat., 3 032 599, 1962.
[2] M. Hino, S. Kobayashi and K. Arata, J. Am. Chem. Soc., 1979, **101,** 6439-6441.
[3] M. Hino and K. Arata, J. Chem. Soc., Chem. Commun., 1980, 851-852.
[4] X. Song and A. Sayari, Catal. Rev. Sci. Eng., 1996, **38**, 329-412.
[5] G. D. Yadav and J. J. Nair, Microporous Mesoporous Mater., 1999, **33**, 1-48.
[6] T. Kimura, Catal. Today, 2003, **81**, 57-63.
[7] F. C. Jentoft, Sulfated Zirconia Alkane Isomerisation Catalysts: A Treatise, Thesis (Habilitationsschrift), Humboldt-Universität Berlin, 2004.
[8] A. Hofmann and J. Sauer, J. Phys. Chem. B, 2004, **108**, 14652-14662.
[9] X. Li, K. Nagaoka, L. J. Simon, R. Olindo, J. A. Lercher, A. Hofmann and J. Sauer, J. Am. Chem. Soc., 2005, **127**, 16159-16166.
[10] J. A. Rodriquez and D. W. Goodman, Surf. Sci. Rep., 1991, **14**, 1-107.
[11] J. Freund, H. Kuhlenbeck and V. Staemmler, Rep. Prog. Phys., 1996, **59**, 283-347.
[12] K. Meinel, A. Hofmann, S. Förster, R. Kulla, K. M. Schindler, H. Neddermeyer, J. Sauer and W. Widdra, Phys. Chem. Chem. Phys., 2006, **8**, 1593-1600.
[13] P. L. J. Gunter, J. W. Niemantsverdriet, F. H. Ribiberteiro, G. A. Somorjai, Catal. Rev. Sci. Eng., 1999, **39**, 77-168.
[14] J. W. Niemantsverdriet, A. F. P. Engelen, A. M. de Jong, W. Wieldraaijer and G. J. Kramer, Appl. Surf. Sci., 1999, **144-145**, 366-374.
[15] H. Shin, M. Agarwal, M. R. De Guire and A. H. Heuer, J. Am. Ceram. Soc., 1996, **79**, 1975-1978.
[16] M. Agarwal, M. R. De Guire and A. H. Heuer, J. Am. Ceram. Soc., 1997, **80**, 2967-2981.
[17] H. Shin, M. Agarwal, M. R. De Guire and A. H. Heuer, Acta Mater., 1998, **46**, 801-815.
[18] T. P. Niesen, M. R. De Guire, J. Bill, F. Aldinger, M. Rühle, A. Fischer, F. C. Jentoft and R. Schlögl, J. Mater. Res., 1999, **14**, 2464-2475.
[19] A. Fischer, F. C. Jentoft, G. Weinberg, R. Schlögl, T. P. Niesen, J. Bill, F. Aldinger, M. R. De Guire and M. Rühle, J. Mater. Res., 1999, **14**, 3725-3733.
[20] F. C. Jentoft, A. Fischer, G. Weinberg, U. Wild and R. Schlögl, Stud. Surf. Sci. Catal., 2000, **130,** 209-214.
[21] A. Fischer, Doctorial Thesis, TU Berlin, 2001.
[22] H. Cölfen, H. Schnablegger, A. Fischer, F. C. Jentoft, G. Weinberg and R. Schlögl, Langmuir, 2002, **18,** 3500-3509.
[23] Y. Tang and M. R. De Gurie, J. Mater. Chem., 2004, **14**, 1173-1179.
[24] A. D. Polli, T. Wagner, A. Fischer, G. Weinberg, F. C. Jentoft, R. Schlögl and M. Rühle, Thin Solid Films, 2000, **379,** 122-127.
[25] V. V. Roddatis, D. S. Su, F. C. Jentoft and R. Schlögl, Philos. Mag. A., 2002, **82,** 2825-2839.
[26] V. V. Roddatis, D. S. Su, E. Beckmann, F. C. Jentoft, U. Braun, J. Kröhnert and R. Schlögl, Surf. Coat. Technol., 2002, **151-152**, 63-66.
[27] J. Wang, S. Yang, X. Liu, S. Ren, F. Guan and M. Chen, Appl. Surf. Sci., 2004, **221**, 272–280.
[28] [1] J. Wang, X. Liu, S. Ren, F. Guan and S. Yang, Tribology Lett., 2005, **18**, 429-436.
[29] G. Zhang, J. Y. Howe, D. W. Coffey, D. A. Blom, L. F. Allard and J. Cho, Mater. Sci. Eng., C, 2006, **26**, 1344–1350.
[30] W. Ranke and Y. Joseph, Phys. Chem. Chem. Phys., 2002, **4**, 2483–2498.
[31] K. Christmann, Introduction to Surface Physical Chemistry, Steinkopff Verlag, Darmstadt, 1991.
[32] S. Fölsch, A. Stock and M. Henzler, Surf. Sci., 1992, **264**, 65-72.
[33] M. Henzler, A. Stock and M. Böl, in Adsorption on Ordered Surfaces of Ionic Solids and Thin Films, ed. E. Umbach and H. J. Freund, Springer, Berlin, 1993, vol. 33., pp. 15-23.
[34] W. Ranke, Surf. Sci., 1995, **342**, 281-292.
[35] W. Ranke and W. Weiss, Surf. Sci., 1998, **414**, 236-253.
[36] W. Ranke and W. Weiss, Surf. Sci., 2000, **465**, 317-330.
[37] Y. Joseph, W. Ranke and W. Weiss, J. Phys. Chem. B, 2000, **104**, 3224-3236.
[38] W. Kern, J. Electrochem. Soc., 1990, **137**, 1887-1892.
[39] J. F. Moulder, W. F. Stickle, P. E. Sobol and K. D. Bomben, Handbook of X-ray Photoelectron Spectroscopy, Perkin Elmer Physical Electrons Division, 1992.
[40] C. D. Wagner, L. E. Davis, M. V. Zeller, J. A. Taylor, R. M. Raymond and L. H. Gale, Surf. Interface Anal., 1981, **3**, 211–225.
[41] W. Weiss, M. Ritter, D. Zscherpel, M. Swoboda and R. Schlögl, J. Vac. Sci. Technol. A, 1998, **16**, 21-29.
[42] N. M. Rodriguez, P. E. Anderson, A. Wootsch, U. Wild, R. Schlögl, and Z. Páal, J. Catal., 2001, **197**, 365-377.
[43] C. Breitkopf, H. Papp, X. Li, R. Olindo, J. A. Lercher, R. Lloyd, S. Wrabetz, F. C. Jentoft, K. Meinel, S. Förster, K. M. Schindler, H. Neddermeyer, W. Widdra, A. Hofmann and J. Sauer, Phys. Chem. Chem. Phys., 2007, **9**, 3600-3618.
[44] M. P. Seah and W. A. Dench, Surf. Interf. Anal., 1979, **1**, 2-11.
[45] P. Kramer and L.J. van Ruyven, Appl. Phys. Lett., 1972, **20**, 420-422.
[46] M. H. Hecht, Phys. Rev. B, 1990, **41**, 7918-7921.

[47] S. Chang, I. M. Vitomirov, L. J. Brillson, D. F. Rioux, P. D. Kirchner, G. D. Pettit, J.M. Woodall and M. H. Hecht, Phys. Rev. B, 1990, **41**, 12299-12302.
[48] K. Kimura, S. Katsumata, Y. Achiba, T. Yamazaki, S. Iwata, Handbook of He I Photoelectron Spectra of Fundamental Organic Molecules, Japan Scientific Societies Press, Tokyo and Halsted Press, New York, 1981.
[49] R. Srinivasan, R. A. Keogh, D. R. Milburn and B. H. Davis, J. Catal., 1995, **153**, 123-130.
[50] R. C. Garvie and M. F. Goss, J. Mater. Sci., 1986, **21**, 1253-1257.
[51] R. C. Garvie, J. Phys. Chem., 1965, **69**, 1238-1243.
[52] R. C. Garvie, J. Phys. Chem., 1978, **82**, 218-224.
[53] A. Christensen and E. A. Carter, Phys. Rev. B, 1998, **58,** 8050-8064.
[54] I. Molodetsky, A. Navrotsky, M. J. Paskowitz, V. J. Leppert and S. H. Risbud, J. Non-Cryst. Solids, 2000, **262**, 106-113.
[55] C. Morterra, G. Poncelet, F. Pinna and M. Signoretto, J. Catal., 1995, **157**, 109-123.
[56] D. Briggs and T. Grant, Surface Analysis by Auger and X-ray Photoelectron Spectroscopy, IM Publications, West Sussex and Surface Spectra Limited, Manchester, 2003.
[57] L. Sanche, Nucl. Instrum. Methods Phys. Res., Sect. B, 2003, **208**, 4-10.
[58] S. E. Hoory and J. M. Prausnitz, Trans. Faraday Soc., 1967, **63**, 455-460.
[59] G. C. Chirnside and C. G. Pope, J. Phys. Chem., 1964, **68**, 2377-2379.
[60] S. Ross, J. K. Salens and J. Olivier, J Phys. Chem., 1962, **66**, 696-700.
[61] S. Wrabetz, X. Yang, G. Tzolova-Müller, R. Schlögl, F.C. Jentoft, J. Catal., 2010, **269**, 351-358.
[62] T. Arnold, S. Channa, S. M. Clarke, R. E. Cook and J. Z. Larese, Phys. Rev. B, 2006, **74**, 085421.
[63] Z. Wu, S. N. Ehrlich, B. Matthies, K. W. Herwig, P. Dai, U. G. Volkmann, F. Y. Hansen and H. Taub, Chem. Phys. Lett., 2001, **348**, 168-174.
[64] J. M. Hilding and E. A. Grulke, J. Phys. Chem. B, 2004, **108**, 13688-13695.
[65] X. Li, K. Nagaoka, L. J. Simon, J. A. Lercher, S. Wrabetz, F. C. Jentoft, C. Breitkopf, S. Matysik and H. Papp, J. Catal., 2005, **230**, 214-225.
[66] M. R. González, K. B. Fogash, J. M. Kobe and J. A. Dumesic, Catal. Today, 1997, **33**, 303-312.
[67] C. Breitkopf, J. Mol. Catal. A: Chem., 2005, **226**, 269–278.
[68] X. Li, K. Nagaoka, L. J. Simon, R. Olindo and J. A. Lercher, J. Catal., 2005, **232**, 456-466.
[69] S. Wrabetz and F. C. Jentoft, unpublished data.
[70] K. B. Fogash, R. B. Larson, M. R. González, J. M. Kobe and J.A. Dumesic, J. Catal., 1996, **163**, 138–147.
[71] N. Katada, J. Endo, K. Notsu, N. Yasunobu, N. Naito and M. Niwa, J. Phys. Chem. B, 2000, **104**, 10321-10328.
[72] D. Briggs and M. P. Seah, Practical Surface Analysis, John Wiley and Sons, Chichester, 2nd edn., 1990, vol. 1, pp. 168-173 and 244-248.
[73] B.S. Klose, F.C. Jentoft, R. Schlögl, I.R. Subbotina, V.B. Kazansky, Langmuir, 2005, **21**, 10564–10572.
[74] R. Lloyd, E. M. Vass, M. Hävecker, F. C. Jentoft and R. Schlögl, in preparation.